

# Structure and Composition of Mixed Surfactant Micelles of Sodium Dodecyl Sulfate and Hexaethylene Glycol Monododecyl Ether and of Hexadecyltrimethylammonium Bromide and Hexaethylene Glycol Monododecyl Ether

J. Penfold,<sup>\*,†</sup> E. Staples,<sup>‡</sup> L. Thompson,<sup>‡</sup> I. Tucker,<sup>‡</sup> J. Hines,<sup>‡</sup> R. K. Thomas,<sup>§</sup> J. R. Lu,<sup>⊥</sup> and N. Warren<sup>§</sup>

*ISIS Facility, Rutherford Appleton Laboratory, Chilton, Didcot, Oxon OX11 0QX, U.K., Unilever Research, Port Sunlight Laboratory, Quarry Road East, Bebington, Wirral L63 3JW, U.K., Physical Chemistry Laboratory, University of Oxford, South Parks Road, Oxford OX1 3QZ, U.K., and Chemistry Department, University of Surrey, Guildford, Surrey GU2 5XH, U.K.*

*Received: February 17, 1999; In Final Form: April 26, 1999*

Small-angle neutron scattering has been used to study the structure and composition of mixed ionic–nonionic surfactant micelles. A comparison between two different mixed surfactant systems, sodium dodecyl sulfate (SDS) and hexaethylene glycol monododecyl ether (C<sub>12</sub>EO<sub>6</sub>) and hexadecyltrimethylammonium bromide (C<sub>16</sub>TAB) and C<sub>12</sub>EO<sub>6</sub>, both in 0.1 M NaCl, has been made. In the latter system, ideal mixing is observed, and in the former, departure from ideality, broadly consistent with regular solution theory, RST, is observed. The deviations from the predictions of RST are attributed to subtle changes in the packing of the two surfactants in the mixed micelles. For the SDS/C<sub>12</sub>EO<sub>6</sub> mixture, the micellar aggregation number is essentially constant with composition and concentration, whereas for the C<sub>16</sub>TAB/C<sub>12</sub>EO<sub>6</sub> mixture there is a marked micellar growth with increasing concentration and mole fraction of C<sub>12</sub>EO<sub>6</sub> in solution. The SANS results on structure and composition are compared with the results reported for other mixed surfactant systems and are discussed in the context of recent theoretical developments.

## Introduction

In the technological, industrial, and domestic applications of surfactants, mixtures are frequently used, either because the commercial surfactants used contain mixtures of different alkyl chain lengths and isomeric forms or because surfactants are deliberately mixed to optimize some aspect of performance.<sup>1</sup> In mixed micellar solutions, it is well-known that physical properties, such as the critical micellar concentration (cmc) and interfacial tension, can be significantly lower than would be expected from the properties of the pure components. This synergism<sup>2</sup> is evidence of nonideal behavior and is an important aspect of the application of surfactant mixtures in their extensive industrial, technological, and domestic applications. Although this synergy has been widely exploited in designing mixtures that display particular desirable properties, the basic processes are still relatively poorly understood at a detailed molecular level.

The ideal solution approach<sup>3</sup> and the subsequent adaptation of regular solution theory (RST),<sup>4,5</sup> where the departure from ideality is parametrized by a single interaction parameter,  $\beta$ , have formed the basis of much of the theoretical effort in this area. More recently, more detailed molecular–thermodynamic theories have been developed,<sup>6–9</sup> which within a thermodynamic framework include molecular detail and specific interactions between the different components. Such theories provide the potential to predict cmc's, micellar compositions, aggregation numbers, and structure.

In parallel, there has been a recent spate of experimental studies using a variety of techniques on micellization in mixed surfactants, using static and dynamic light scattering,<sup>10</sup> neutron scattering,<sup>11–13</sup> NMR<sup>14</sup> fluorescence quenching, and a variety of different techniques.<sup>15</sup>

We have previously shown that neutron reflectivity and small-angle neutron scattering (SANS), in combination with H/D isotopic substitution, can provide information on surface and micellar compositions in mixed surfactant solutions over a wide range of compositions and concentrations, and this has been demonstrated for a range of different mixtures.<sup>16–19</sup> Furthermore, we have shown that neutron reflectivity can provide detailed structural information on an adsorbed mixed surfactant layer at the interface,<sup>20,21</sup> and the correlation between structural changes and composition has been established. It is also well-established that SANS is an excellent probe of the micelle structure,<sup>22</sup> and this has also been demonstrated for mixed surfactant micelles.<sup>11–13</sup> However, there has been no detailed study using SANS, where the possible correlation between structure and composition has been investigated.

We have recently used SANS and neutron reflectivity<sup>11</sup> to study the adsorption and micellization of the mixed nonionic–anionic surfactant system, sodium dodecyl sulfate (SDS)/*n*-dodecylhexaethylene glycol (C<sub>12</sub>EO<sub>6</sub>) in 0.1 M NaCl. The composition of the surfactant layer adsorbed at the air–solution interface was compared with the micellar composition over a wide concentration range, and the results were found to be broadly consistent with the predictions of regular solution theory. In this paper, we will extend the initial study on the SDS/C<sub>12</sub>EO<sub>6</sub> mixtures<sup>11</sup> with more extensive measurements on the composition of the structure of two ionic/nonionic mixed

\* Address all correspondence to Dr. J. Penfold.

<sup>†</sup> Rutherford Appleton Laboratory.

<sup>‡</sup> Port Sunlight Laboratory.

<sup>§</sup> University of Oxford.

<sup>⊥</sup> University of Surrey.

surfactant (both in 0.1 M NaCl), SDS/C<sub>12</sub>EO<sub>6</sub> and C<sub>12</sub>EO<sub>6</sub>/hexadecyltrimethylammonium bromide (C<sub>16</sub>TAB) micelles. The aim of the study is to correlate the changes in the micelle structure and aggregation number with composition and any departure from ideal mixing. To establish this correlation, measurements have been made over a wide range of solution compositions and concentrations for both surfactant mixtures.

### Experimental Details

Measurements of the micelle structure and composition were made for SDS/C<sub>12</sub>EO<sub>6</sub> in 0.1 M NaCl in the concentration range  $3 \times 10^{-4}$  to  $10^{-2}$  M for solution compositions of 70:30, and 50:50, 30:70, and 5:95 (mol %) SDS/C<sub>12</sub>EO<sub>6</sub> in 0.1 M NaCl and for C<sub>12</sub>EO<sub>6</sub>/C<sub>16</sub>TAB in 0.1 M NaBr in the concentration range  $2.5 \times 10^{-4}$  to 0.1 M for solution compositions of 70:30, 50:50, and 25:75 (mol %) C<sub>12</sub>EO<sub>6</sub>/C<sub>16</sub>TAB. The surfactant molarities quoted throughout the paper refer to the total surfactant concentration. All solutions were prepared in deuterium oxide (D<sub>2</sub>O). For the SDS/C<sub>12</sub>EO<sub>6</sub> mixtures, measurements were made with both surfactants protonated, h-SDS/h-C<sub>12</sub>EO<sub>6</sub>, and with the SDS deuterated, d-SDS/h-C<sub>12</sub>EO<sub>6</sub>, and some limited measurements were made with the other labeled combination, h-SDS/d-C<sub>12</sub>-h-EO<sub>6</sub>. For C<sub>12</sub>EO<sub>6</sub>/C<sub>16</sub>TAB, the measurements were made with both surfactants protonated, h-C<sub>12</sub>EO<sub>6</sub>/h-C<sub>16</sub>-h-TAB, and with the C<sub>16</sub>TAB deuterium labeled, h-SDS/d-C<sub>16</sub>-h-TAB, and some limited measurements were made with the other labeled combination, d-C<sub>12</sub>-h-EO<sub>6</sub>/h-C<sub>16</sub>-h-TAB. (See note below on the description of the labeling nomenclature used in this paper.)

The protonated surfactants were obtained from Nikkol (h-C<sub>12</sub>EO<sub>6</sub>) and BDH (h-SDS). The deuterium-labeled compounds were synthesized, purified, and characterized at the Physical Chemistry Laboratory at the University Oxford by Thomas's group using methods described previously.<sup>23,24</sup> The chemical purity of all the surfactants was assessed by surface tension measurements and TLC and used without further purification. Deuterium oxide was supplied by Flourochem, and high-purity water (Elga Ultrapure) was used throughout. All glassware and sample cells were cleaned using alkaline detergent (Decon 90), followed by copious washing in high-purity water. All samples were measured in Hellma quartz spectrophotometer cells.

The SANS measurements were made on the LOQ diffractometer<sup>25</sup> at the ISIS pulsed neutron source at the Rutherford Appleton Laboratory and on the D17 and D22 diffractometers at the Institute Laue Langevin, Grenoble.<sup>26</sup> On the LOQ, the measurements were made using the white-beam time-of-flight method with a limited wavelength range at a source frequency of 50 Hz (giving a  $Q$  range of 0.02–0.15 Å<sup>-1</sup>). A beam aperture of 12 mm and a sample path length of 5 mm were used, and the samples were measured at a temperature of 30 °C. The measurements on the D17 were made at a fixed wavelength ( $\lambda$ ) of 9 Å ( $\Delta\lambda/\lambda$  of 10%) and a sample-to-detector distance of 2.8 m to give a  $Q$  range of 0.026–0.08 Å<sup>-1</sup>. The measurements on the D22 were made at a fixed wavelength of 8 Å and a sample-to-detector distance of 8.0 m to give a  $Q$  range of 0.01–0.1 Å<sup>-1</sup>. Five-millimeter path length cells were used on the D17 and 2 mm on the D22. The instrument configurations and sample geometries were optimized to give maximum sensitivity to surfactant concentrations close to the cmc, over a limited  $Q$  range.

**Note on Labeling Nomenclature.** d-SDS and h-SDS are CD<sub>3</sub>(CD<sub>2</sub>)<sub>11</sub>OSO<sub>3</sub>Na and CH<sub>3</sub>(CH<sub>2</sub>)<sub>11</sub>OSO<sub>3</sub>Na, h-C<sub>12</sub>EO<sub>6</sub> and d-C<sub>12</sub>-h-EO<sub>6</sub> are CH<sub>3</sub>(CH<sub>2</sub>)<sub>11</sub>(OCH<sub>2</sub>CH<sub>2</sub>)<sub>6</sub>OH and CD<sub>3</sub>(CD<sub>2</sub>)<sub>11</sub>-(OCH<sub>2</sub>CH<sub>2</sub>)<sub>6</sub>OH, and h-C<sub>16</sub>-h-TAB and d-C<sub>16</sub>-h-TAB are CH<sub>3</sub>-(CH<sub>2</sub>)<sub>15</sub> N(CH<sub>3</sub>)Br and CD<sub>3</sub>(CD<sub>2</sub>)<sub>15</sub>N(CH<sub>3</sub>)<sub>3</sub>BR.

The data from all three diffractometers were corrected for background scattering and detector responses and converted to scattering cross sections (in absolute units of cm<sup>-1</sup>) using standard procedures.<sup>27,28</sup>

The scattering cross section for colloidal particles in a solution can be written as<sup>22</sup>

$$\frac{d\sigma}{d\Omega} = N \left| \int_V (\rho_p(r) - \rho_s) \exp(iQr) d^3r \right|^2 \quad (1)$$

where  $\rho_p$  and  $\rho_s$  are the particles of solvent scattering length densities and  $N$  is the number of particles per unit volume.

For spherical monodisperse micelles in solution,<sup>23</sup> then

$$\frac{d\sigma}{d\Omega} \approx NP(Q) S(Q) \quad (2)$$

where  $N$  is now the micelle number density,  $P(Q)$  is the particle form factor  $P(Q) = 3(\sin(QR) - QR \cos(QR))/(QR)^3/3$  where  $R$  is the particle radius, and  $S(Q)$  is the interparticle structure factor arising from the inter-micellar interactions in the solution.

For a dilute solution of mixed surfactant micelles in the limit of small  $Q$ , where  $P(Q) \approx S(Q) \approx 1.0$ , the scattered intensity can be written as

$$I(Q) \propto \sum_i N_i V_i^2 (\rho_{ip} - \rho_s)^2 \quad (3)$$

where  $N$  is the micelle number density,  $V$  is the micelle "dry" volume,  $\rho_p$  is the micelle scattering length density,  $\rho_s$  is the solvent scattering length density, and the summation is over all micelle compositions for the binary surfactant mixture.

By making two different measurements, one with both surfactants protonated and a second with one of the surfactants deuterated, the ratio of the two measured intensities, extrapolated to  $Q = 0$ , gives directly an estimate of the micellar composition. For example (see ref 11), for the combinations of h-SDS/h-C<sub>12</sub>-h-EO<sub>6</sub> and h-SDS/d-C<sub>12</sub>-h-EO<sub>6</sub> in D<sub>2</sub>O, the volume and mole fractions of C<sub>12</sub>EO<sub>6</sub> in the micelles are given by

$$V_f = \frac{(\sqrt{R_1} - 1)(\rho_{h-SDS} - \rho_{D_2O})}{(\rho_{h-C_{12}E_6} - \rho_{h-SDS}) - \sqrt{R_1}(\rho_{d-C_{12}E_6} - \rho_{h-SDS})} \quad (4)$$

and

$$M_f = \frac{V_f/V_{C_{12}E_6}}{V_f/V_{C_{12}E_6} + (1 - V_f)/V_{SDS}} \quad (5)$$

and where  $V_f$  and  $M_f$  are the volume and mole fraction of C<sub>12</sub>-EO<sub>6</sub> in the micelles,  $R_1$  the intensity ratio  $I_{h-SDS/h-C_{12}E_6}/I_{h-SDS/d-C_{12}E_6}$  (at  $Q = 0$ ),  $\rho_i$  the scattering length density of component  $i$ ,  $I_i$  the scattered intensity (at  $Q = 0$ ) for system  $i$ , and  $V_i$  the molecular volume of component  $i$ .

For such SANS measurements, instrumentally related systematic variations, such as detector response and calibration errors, introduce errors in the determination of the absolute scattering cross sections that are typically ~10%. However, in determining the micelle composition from the intensity ratio in eq 4 and assuming that the composition distribution is narrow, many of these uncertainties cancel such that the error in the composition is typically ~1%. Mixed micelles can, of course, have large composition fluctuations. From eq 3, it can be seen that the different isotopic labeling schemes used will reflect the different components of the micelle composition distribution, and this will result in a small error in the deduced micelle

**TABLE 1: Micelle Compositions for SDS/C<sub>12</sub>EO<sub>6</sub>**

soln	concn, M	mole % (SDS)
70/30	10 <sup>-2</sup>	0.69 ± 0.015
	5 × 10 <sup>-3</sup>	0.68
	2 × 10 <sup>-3</sup>	0.62
	1.25 × 10 <sup>-3</sup>	0.61 ± 0.02
	10 <sup>-3</sup>	0.53
	6.25 × 10 <sup>-4</sup>	0.5 ± 0.06
50/50	3.13 × 10 <sup>-4</sup>	0.395 ± 0.005
	10 <sup>-2</sup>	0.51 ± 0.016
	5 × 10 <sup>-3</sup>	0.53
	2.5 × 10 <sup>-3</sup>	0.50
30/70	1.25 × 10 <sup>-3</sup>	0.44 ± 0.04
	6.25 × 10 <sup>-4</sup>	0.38 ± 0.04
	10 <sup>-2</sup>	0.29 ± 0.01
	5 × 10 <sup>-3</sup>	0.28
20/80	2.5 × 10 <sup>-3</sup>	0.27
	10 <sup>-3</sup>	0.25
	5 × 10 <sup>-4</sup>	0.21
	1.25 × 10 <sup>-3</sup>	0.16 ± 0.01
5/95	6.25 × 10 <sup>-4</sup>	0.13 ± 0.015
	3.1 × 10 <sup>-4</sup>	0.13 ± 0.01
	1.25 × 10 <sup>-3</sup>	0.05 ± 0.015

**TABLE 2: Micelle Compositions for C<sub>16</sub>TAB/C<sub>12</sub>EO<sub>6</sub>**

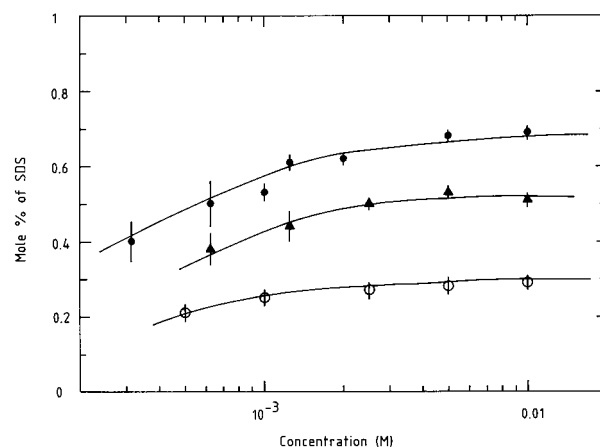
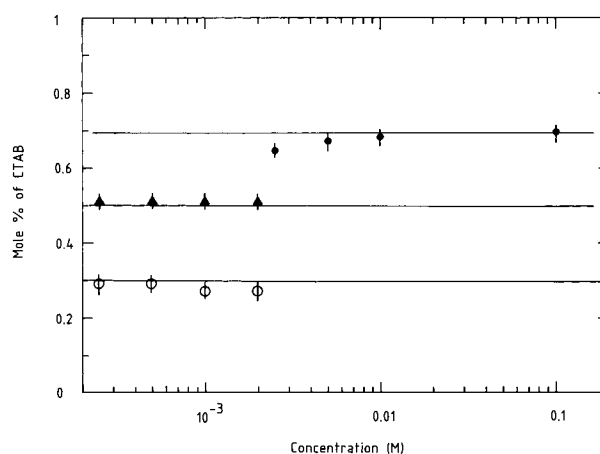
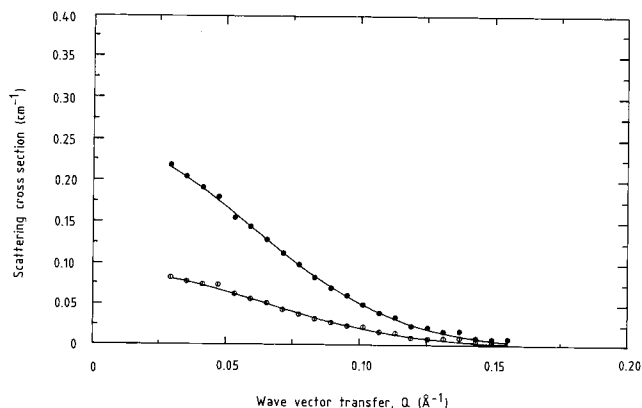
soln	concn, M	mol % (C <sub>16</sub> TAB)
70/30	10 <sup>-1</sup>	0.70 ± 0.02
	10 <sup>-2</sup>	0.69
	5 × 10 <sup>-3</sup>	0.68
	2.5 × 10 <sup>-3</sup>	0.67
50/50	2 × 10 <sup>-3</sup>	0.51 ± 0.02
	10 <sup>-3</sup>	0.51
	5 × 10 <sup>-4</sup>	0.51
	2.25 × 10 <sup>-4</sup>	0.51
25/75	2 × 10 <sup>-3</sup>	0.27 ± 0.02
	10 <sup>-3</sup>	0.27
	5 × 10 <sup>-4</sup>	0.29
	2.5 × 10 <sup>-4</sup>	0.29

compositions. By including a distribution in the calculation of composition, we have shown<sup>11</sup> that this error can be evaluated, as in the limit of high concentration the true micelle composition must approach that of the solution. In some of the data presented in this paper,  $S(Q) \neq 1.0$ , so eq 4 is not strictly correct. However, as  $S(Q)$  should not vary with the isotopic content and providing the data obtained can be effectively extrapolated to small  $Q$  (where  $P(Q) \sim 1.0$ ), the contribution from  $S(Q)$  should cancel in the ratio of intensities ( $R_1$ ). We have verified this by making some of the measurements with the complementary combinations of hh/dh and hh/hd, which within error give the same composition, and by detailed modeling (including the composition as an additional variable) of the different isotopically labeled combinations (see, for example, Table 7 and Figure 5).

The micelle structure was established by analyzing the scattering data using a standard and now well-established model for micelles.<sup>22</sup> For a solution of globular polydisperse interacting particles, the coherent scattering cross section can be written by the so-called “decoupling approximation” (assuming that there are no correlations between position, orientation, and size)<sup>22,29</sup>

$$\frac{d\sigma}{d\Omega_{\text{coh}}} = N_p [S(Q) \langle |F(Q)|^2 \rangle + \langle |F(Q)|^2 \rangle - \langle |F(Q)| \rangle^2] \quad (6)$$

where the averages denoted by  $\langle \rangle$  are averages over the particle size and orientation.  $N_p$  is the particle number density,  $S(Q)$  the structure factor, and  $F(Q)$  the particle form factor. The micelles are modeled as a “core + shell”,<sup>22</sup> and hence, the form factor is

**Figure 1.** Mole % SDS as a function of solution composition for SDS/C<sub>12</sub>EO<sub>6</sub> mixed micelles: (●) 70/30, (▲) 50/50, and (○) 30/70. The solid lines are RST calculations for  $\beta_m = -2.58$  (for 70/30) and  $\beta_m = -1.96$  (for 50/50 and 30/70).**Figure 2.** Mole % C<sub>16</sub>TAB as a function of solution composition for C<sub>16</sub>TAB/C<sub>12</sub>EO<sub>6</sub> mixed micelles: (●) 70/30, (▲) 50/50, and (○) 25/75.**Figure 3.** SDS/C<sub>12</sub>EO<sub>6</sub> (50/50); 0.1 M NaCl, 2.5 × 10<sup>-3</sup> M hh (●) and dh (○) in D<sub>2</sub>O.

$$F(Q) = V_1(\rho_1 - \rho_2)F_0(QR_1) + V_2(\rho_2 - \rho_s)F_0(QR_2) \quad (7)$$

where  $V_i = 4\pi R_i^3/3$ ,  $F_0(QR) = 3j_1(QR)/(QR)$ , and  $\rho_1$ ,  $\rho_2$ , and  $\rho_s$  are the scattering length densities of the micelle core and shell and of the solvent.

The inner core, made up of the alkyl chains only, is constrained to space fill a volume limited by a radius  $R_1$  and defined by the fully extended chain length of the surfactant (note that for the C<sub>16</sub>TAB/C<sub>12</sub>EO<sub>6</sub> mixtures where the chain lengths

**TABLE 3: Indication of Spread in Values (from Repeated Measurements)**

$10^{-2}$ M	70/30	SDS/C <sub>12</sub> EO <sub>6</sub>	0.69, 0.70, 0.68, 0.69, 0.67, 0.72, 0.68, 0.70, 0.66
$1.25 \times 10^{-3}$ M	70/30	SDS/C <sub>12</sub> EO <sub>6</sub>	0.63, 0.62, 0.61, 0.51, 0.54, 0.57, 0.54, 0.54

**TABLE 4: Calculated Variation in the Mean Micellar Composition for a 70/30 Mixture of SDS/C<sub>12</sub>EO<sub>6</sub> for Different Widths of a Schultz Composition<sup>11</sup> Distribution Function at  $10^{-3}$  M and in 0.1 M NaCl<sup>a</sup>**

$\sigma$	mol % SDS in micelles
0.0	0.69
0.02	0.695
0.05	0.70
0.1	0.71
0.15	0.74

<sup>a</sup> The theoretical work of Barzykin and Almgren<sup>49</sup> on the distribution of surfactants in mixed micelles composition is consistent with a log-normal or Schultz distribution of composition in a binary mixture.

**TABLE 5: Model Parameters from Structural Determination for SDS/C<sub>12</sub>EO<sub>6</sub>**

comp	surf concn, (M)	salt concn, (M)	agg	z	$R_1, \text{\AA}$	$R_2$	alf	ee	poly
70/30	$10^{-2}$	0.1	92	2.4	16.7	24.7	0.65	1.0	0.12
	$5 \times 10^{-3}$	0.1	97	2.1	16.7	25.3	0.60	1.0	0.12
	$2 \times 10^{-3}$	0.1	86	1.0	16.7	24.0	0.64	1.0	0.12
	$1.25 \times 10^{-3}$	0.1	92	2.3	16.7	25.2	0.60	1.0	0.12
	$10^{-3}$	0.1	83	1.0	16.7	27.2	0.71	1.0	0.12
50/50	$10^{-2}$	0.1	100	2.3	16.7	25.5	0.59	1.0	0.12
	$5 \times 10^{-3}$	0.1	100	2.3	16.7	25.5	0.59	1.0	0.12
	$2.5 \times 10^{-3}$	0.1	95	2.0	16.7	25.2	0.62	1.0	0.12
	$1.25 \times 10^{-3}$	0.1	96	0.0	16.7	25.2	0.62	1.0	0.12
	$6.25 \times 10^{-4}$	0.1	104	0.0	16.7	25.7	0.57	1.0	0.12
30/70	$10^{-2}$	0.1	97	1.0	16.7	25.7	0.61	1.0	0.12
	$5 \times 10^{-3}$	0.1	97	1.0	16.7	25.7	0.61	1.0	0.12
	$2.5 \times 10^{-3}$	0.1	91	1.0	16.7	25.2	0.65	1.0	0.12
	$10^{-3}$	0.1	88	1.0	16.7	25.1	0.67	1.0	0.12
	$1.25 \times 10^{-3}$	0.1	155	0.0	16.7	24.0	1.0	2.6	0.0
70/30	$1.43 \times 10^{-2}$	0.01	64	8.5	16.7	22.8	0.93	1.0	0.15
	$7.15 \times 10^{-3}$	0.01	63	6.0	16.7	23.3	0.94	1.0	0.15
	$3.38 \times 10^{-3}$	0.01	60	6.0	16.7	21.8	1.0	1.0	0.15

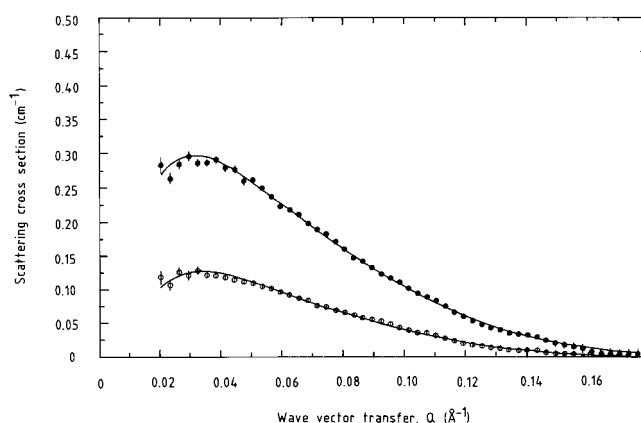
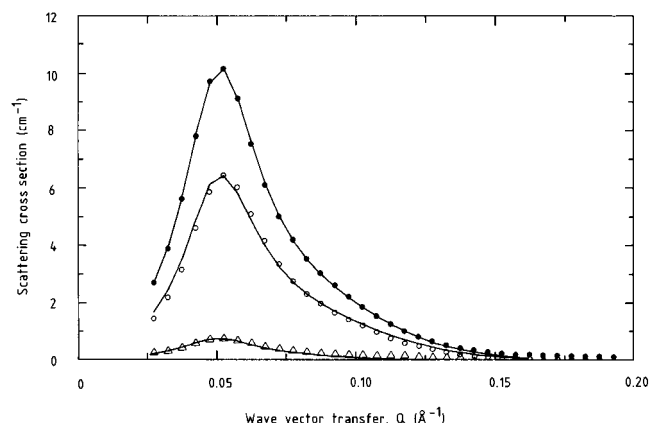
**TABLE 6: Model Parameters from Structural Determination for C<sub>16</sub>TAB/C<sub>12</sub>EO<sub>6</sub>**

comp	surf concn, (M)	salt concn, (M)	agg	z	$R_1, \text{\AA}$	$R_2$	alf	ee	poly
70/30	$10^{-1}$	0.1	150	19.3	19.9	25.4	1.0	1.8	0.0
	$10^{-2}$		135	1.0	19.9	25.4	1.0	1.6	0.0
	$5 \times 10^{-3}$		113	1.0	19.9	25.4	1.0	1.4	0.0
	$2.5 \times 10^{-3}$		105	1.0	19.9	25.4	1.0	1.3	0.0
	$2 \times 10^{-3}$	0.1	258	0.0	19.0	25.1	1.0	3.3	0.0
50/50	$10^{-3}$		216	0.0	19.0	25.1	1.0	2.8	0.0
	$5 \times 10^{-4}$		124	0.0	19.0	29.5	0.6	1.0	0.15
	$2.5 \times 10^{-4}$		124	0.0	19.0	29.5	0.6	1.0	0.15
	$2 \times 10^{-3}$	0.1	229	0.0	17.9	24.6	1.0	3.3	0.0
	$10^{-3}$		197	0.0	17.9	24.6	1.0	2.6	0.0
25/75	$5 \times 10^{-4}$		157	0.0	17.9	25.6	1.0	2.3	0.0
	$2.5 \times 10^{-4}$		101	0.0	17.9	28.1	0.7	1.0	0.15

of the two surfactants are different,  $R_1$  is taken as the volume fraction weighted mean of the two chain lengths). Any remaining alkyl chain (1-alf), headgroups, and corresponding hydration

**TABLE 7: Model Parameters for Selected Detailed Fits at Different Contrasts**

	contrast	agg	z	$R_1, \text{\AA}$	$R_2$	alf	ee	poly	sf
$10^{-1}$ M 70/30 C <sub>16</sub> TAB/C <sub>12</sub> EO <sub>6</sub> /0.1 M NaCl	hh/D <sub>2</sub> O	150	21.0	19.9	25.4	1.0	1.78	0.0	0.99
	dh/D <sub>2</sub> O								0.91
	dh/H <sub>2</sub> O								1.02
	hh/D <sub>2</sub> O	91	3.3	16.7	24.5	0.86	1.0	0.12	1.02
$10^{-2}$ M 70/30 SDS/C <sub>12</sub> EO <sub>6</sub> /0.1 M NaCl	dh	80	1.6	16.7	23.5	0.73	1.0	0.12	1.15
	hd	87	2.1	16.7	24.1	0.69	1.0	0.12	0.85

**Figure 4.** SDS/C<sub>12</sub>EO<sub>6</sub> (70/30) in 0.01M NaCl hh (●) and hd (○) in  $7.15 \times 10^{-3}$  M D<sub>2</sub>O.**Figure 5.** C<sub>16</sub>TAB (0.1 M; 70/30)/C<sub>12</sub>EO<sub>6</sub>/NaCl (0.1 M), hh (●) and dh (○) in D<sub>2</sub>O and dh (Δ) in H<sub>2</sub>O, showing the best fits to ellipses.

define the radius of the outer shell,  $R_2$ . Polydispersity is included using a Schultz size distribution of micelles sizes,<sup>29</sup> which is a convenient distribution whose form is closely associated with the accepted theoretical forms of micelle polydispersity. The interparticle interactions are included using the RMSA calculation<sup>30,31</sup> for a repulsive Yukawa potential. The adjustable model parameters are then the aggregation number (agg), surface charge (z) (or potential), and polydispersity (poly). The micelle composition is fixed from the values obtained from eqs 4 and 5, and the model is adjusted according to that composition. The model was convoluted with the known instrument resolution and compared with the data on an absolute intensity scale on a least-squares basis. Acceptable model fits require not only that the shape of the scattering is reproduced but that the absolute value of the scattering cross section is in agreement. This is reflected in the value of the scale factor, sf (data/theory), in Tables 5–7, and the acceptable variation is  $\sim \pm 10\%$ . Although most of the data presented in this paper are consistent with the



polydisperse core and shell model of the spherical micelles, the data for the C<sub>16</sub>TAB/C<sub>12</sub>EO<sub>6</sub> mixed micelles (especially at the higher concentrations) are best described using a modified description where the micelles are no longer spherical but elliptical (prolate ellipses). A core and shell description is retained, the dimensions are constrained in the same way as the spherical micelles,<sup>29</sup> and the short dimension of the elliptic inner core now corresponds to  $R_1$ . The ellipticity is characterized by the parameter  $ee$  (see Tables 5–7).

## Results and Discussion

**Micelle Compositions.** We have measured the micelle compositions of two contrasting ionic/nonionic mixed surfactant systems in added electrolyte, over a wide range of concentrations and compositions. We have previously shown<sup>19</sup> that the cationic–nonionic mixture of C<sub>16</sub>TAB–C<sub>12</sub>EO<sub>6</sub> exhibits close to ideal mixing in micelles and at the air–water interface, whereas the anionic–nonionic mixture of SDS–C<sub>12</sub>EO<sub>6</sub><sup>11</sup> nonideally mixes in the micelles and at the air–water interface and is broadly consistent with the predictions of RST. The micelle compositions for both surfactant mixtures, over a wide range of concentrations and compositions, are summarized in Tables 1–3 and plotted in Figures 1 and 2. For the SDS/C<sub>12</sub>EO<sub>6</sub> mixture, the micelle composition evolves with increasing concentration from a composition rich in the more surface-active component (C<sub>12</sub>EO<sub>6</sub> in this case) and tends toward the solution composition in the limit of high concentrations. The solid lines in Figure 1 are calculated from RST (using measured surface tension values for each surfactant and the mixture and an interaction parameter,  $\beta_m$ , of  $-2.7^{11}$ ). The data are broadly consistent with the predictions of RST, but there are some systematic deviations at lower surfactant concentrations and on the values obtained in the limit of high surfactant concentrations. Small errors in the surface tension values can result in large errors in the interaction parameter and, hence, the composition curves, and this has been discussed in detail by us<sup>11</sup> and Hoffman and Poesnecker.<sup>32</sup> In the limit of high concentrations, the micelle composition must be identical to the solution composition, and any deviation can be attributed to a skewed distribution of micelle compositions, as previously described.<sup>11</sup> Table 3 shows the spread in compositions obtained from a series of different independent measurements at two different concentrations and gives an indication of the contribution of systematic errors, which at higher concentrations is  $\sim \pm 0.02$  in composition. Table 4 summarizes the variation in composition that can be obtained by assuming increasingly skewed distributions, and provided the distribution of composition is not grossly anisotropic, the error it introduces in the determination of the micelle composition is of the same order as the systematic errors in the measurement. The deviations at lower concentrations are more significant and are not consistent with a single interaction parameter. A variation in  $\beta_m$  from  $-1.96$  to  $-2.58$ , see solid lines in Figure 1, is required to reproduce the observed variation in the measured composition. The measured micelle compositions are only consistent with the predictions of RST provided  $\beta_m$  is allowed to vary with composition. For a solution composition of 70/30,  $\beta_m$  is  $\sim -2.5$ , whereas for 50/50 and 30/70 it is  $\sim -2.0$ . This suggests that the solution is less ideal the richer it is in SDS. This can be rationalized in terms of the increase in non-zero excess entropy of mixing, due to the greater interaction between SDS molecules within the micelles, resulting in greater packing constraints and the possibilities of changes in hydration. These changes, however, must be sufficiently small as they do not (within the sensitivity of these measurements)

result in a measurable change in the structure of the mixed micelles that are formed (see later).

Variations in  $\beta_m$  with composition have been reported elsewhere. Recently, Hines et al.,<sup>33</sup> from the application of the pseudophase separation model to surface tension data from strongly interacting mixtures of SDS and dodecyl (dimethylamino)acetate (C<sub>12</sub> betaine), have reported similar variations in  $\beta_m$  with solution composition and temperature that have been attributed to changes in hydration. Similar trends were also reported by the same authors for the surfactant mixture of SDS and *n*-dodecyl- $\beta$ -D-maltoside (C<sub>12</sub> maltoside)<sup>34</sup> with a  $\beta_m$  and variation with concentration and composition similar to that reported here for SDS/C<sub>12</sub>EO<sub>6</sub>.

Baglioni et al.<sup>35</sup> have used electron spin–echo modulation of  $\alpha$ -doxylstearic acid spin probe to investigate local packing in the mixed micelles of SDS/C<sub>12</sub>EO<sub>6</sub> and DTAC (dodecyltrimethylammonium chloride)/C<sub>12</sub>EO<sub>6</sub>. From a detailed analysis, they obtained the positions of the DTAC and SDS headgroups relative to the ethylene oxide region of the nonionic surfactant in the mixed micelle at molecular resolution (at a level of resolution not obtainable from SANS). They showed that the DTAC headgroup is located close to the hydrophobic core, whereas the SDS headgroup is in the hydrophilic region close to the micelle surface. The addition of SDS to C<sub>12</sub>EO<sub>6</sub> to form mixed micelles opens up the ethylene oxide region, resulting in increased hydration, which is a maximum for the equimolar mixture. A similar effect is not observed for the C<sub>12</sub>EO<sub>6</sub>/DTAC mixed micelles. Our results for SDS/C<sub>12</sub>EO<sub>6</sub> on the variation of  $\beta$  with composition are consistent with the observations of Baglioni et al. and reinforce the conjecture about the role of hydration.

Shiloach and Blankschtein<sup>9</sup> have developed a molecular model of mixed micellization which retains a thermodynamic framework. The molecular model accounts for micellar mixing nonidealities resulting from electrostatic and steric interactions between headgroups and packing constraints in the micellar cores. Their model predicts the cmc,  $\beta_m$ , micelle and monomer compositions, monomer concentrations, and micelle shape, size, and size distribution. A comparison with our earlier reported SDS/C<sub>12</sub>EO<sub>6</sub> SANS data<sup>11</sup> gave a predicted  $\beta_m$  of  $-3.7$ , in reasonable agreement with our values of  $\beta_m$ . Given a single  $\beta_m$ , the agreement between the data and their theory is worse at the higher SDS compositions. Their calculations show that at micelle compositions  $< 50$  mol % SDS, the free energy is dominated by the electrostatic interactions between the SDS headgroups.

The development of surfactant-selective electrodes<sup>36,37</sup> has provided a suitable method for determining monomer ionic surfactant concentrations. Davidson<sup>36</sup> applied this approach to a range of different surfactant mixtures, included SDS/C<sub>12</sub>EO<sub>6</sub> in 0.2 M NaBr. From an application of the regular solution approximation for surfactant mixing with micelles, they show that

$$\ln \alpha_i^s = \frac{\beta}{RT} (1 - x_i^m)^2 + \ln x_i^m + \left( \mu_{oi}^m - \frac{\mu_i^{os}}{RT} \right) \quad (8)$$

where  $\alpha_i^s$  is the activity of  $i$  in the solution phase,  $x_i^m$  the mole fraction of component  $i$  in the mixed micelle, and  $\mu_{oi}^{m(s)}$  the standard chemical potential of  $i$  in the micellar (solution) phase. Equation 8 predicts that if a mixed micelle is consistent with RST, then a plot of  $\ln(\alpha_i^s/x_i^m)$  against  $(1 - x_i^m)^2$  should be a straight line of slope  $\beta/RT$ . For SDS/C<sub>12</sub>EO<sub>6</sub>, Davidson found a significant departure from such a linear dependence, which

was interpreted as a departure from regular mixing. We have recast the SDS/C<sub>12</sub>EO<sub>6</sub> data of Davidson into a form where we can make a direct comparison with our SDS/C<sub>12</sub>EO<sub>6</sub> data. From the pseudophase approximation, the gradient of  $\ln(\alpha_i^s/x_i^m)$  against  $(1 - x_i^m)^2$  is given by  $\beta_m + x_i^m(d\beta_m/dx_{im})$ , where  $\beta_m$  is any function of  $x_i^m$  and not associated with any model. Applying this to Davidson's data for SDS/C<sub>12</sub>EO<sub>6</sub> implies a  $\beta_m$  that varies from  $-2$  at low SDS solution compositions to  $-10$  in the presence of significant amounts of SDS as reported here. Using RST to calculate the SDS monomer concentrations with a  $\beta_m$  of  $-2.5$  and the known cmc's produces SDS monomer concentrations that are much higher than those inferred from Davidson's data. This implies that Davidson's data are inconsistent with our data for the same system, and without further information, such as the SDS monomer concentrations at the cmc or the nonionic monomer concentrations, it is difficult to pursue the comparison any further. However, considering the advances in surfactant-selective electrodes<sup>37</sup> since the pioneering work of Davidson, it would be interesting to combine the scattering data with new data from surfactant-selective electrode measurements.

In contrast to the SDS/C<sub>12</sub>EO<sub>6</sub> mixtures, we have already shown that the cationic–nonionic mixture of C<sub>16</sub>TAB/C<sub>12</sub>EO<sub>6</sub> in electrolyte behaves as though it is ideally mixing in the micelles.<sup>19</sup> As the interaction parameter is close to zero and the cmc's of the two surfactant constituents are very similar (in 0.1 M NaCl for SDS/C<sub>12</sub>EO<sub>6</sub> and 0.1 M NaBr for C<sub>16</sub>TAB/C<sub>12</sub>EO<sub>6</sub>), for there is now little variation in the micelle composition with concentration (see Figure 2). The variation in micelle composition for the solution mixture of 70/30 C<sub>16</sub>TAB/C<sub>12</sub>EO<sub>6</sub> shows a slightly greater variation in the concentration than in the other two compositions, consistent with a slightly negative interaction parameter and the C<sub>16</sub>TAB cmc being lower than that of C<sub>12</sub>EO<sub>6</sub> in electrolyte. The micelles formed at compositions more rich in C<sub>12</sub>EO<sub>6</sub> are closer to the composition corresponding to the minimum energy micelle formation and show little or no variation in composition with concentration, as discussed in ref 19.

From pulsed gradient spin–echo NMR, PGSE NMR, Griffiths et al.<sup>38</sup> have observed ideal mixing in the sugar-based nonionic surfactant (dodecyl malonobis(*N*-methylglucamide) and SDS micelles. By using the same technique, Ciccarelli et al.<sup>39</sup> have investigated the mixed anionic–nonionic micelles of sodium hexasulfonate (C<sub>6</sub>SNa) and pentaethylene glycol monohexyl ether (C<sub>6</sub>EO<sub>5</sub>). They have interpreted their results for micellar compositions in terms of regular solution theory and report a variation in  $\beta$  with increasing micellar concentration, which they attribute to the contribution of inter-micellar interactions. Although we observe a variation in  $\beta$  with solution composition, we have found no variation in  $\beta$  that could be attributed to inter-micellar interactions. Hassan et al.<sup>40</sup> used the phase separation mode to evaluate surface tension and fluorescence data on C<sub>16</sub>TAB/C<sub>12</sub>EO<sub>6</sub> mixtures. In the absence of electrolyte, they obtained a  $\beta_m$  of  $-3.0$  and found that the variation of cmc with composition was consistent with the regular solution model and a single interaction parameter.

**Micelle Structure.** The structures of the mixed surfactant micelles of SDS/C<sub>12</sub>EO<sub>6</sub> and C<sub>12</sub>EO<sub>6</sub>/C<sub>16</sub>TAB have been evaluated over the same concentration and composition range as the micellar compositions were determined, and the model parameters are summarized in Tables 5–7. The model parameters are a result of a least-squares fit to the data for the different labeling schemes used (see Experimental Section) using the core and

shell model described earlier in the paper. In Table 7, we show the variation in model parameters from the fits to the different “contrasts” measured for the two different mixed surfactant systems at a single concentration and solution composition. This gives an indication of the spread of values and, hence, errors associated with the mean values quoted in Tables 5 and 6.

For the mixture SDS/C<sub>12</sub>EO<sub>6</sub>, the data are well-represented by this model which is composed of polydisperse spheres with an internal core and shell structure. Typical fits to the data for two different compositions and concentrations are shown in Figures 3 and 4. Over the concentration and composition range measured, the micelle size and shape are broadly invariant, and the aggregation number is  $\sim 100$ . The increasing structure in the data is evidence of increased repulsive inter-micellar interactions with increasing SDS content. Douglas and Kaler,<sup>41</sup> in a related study, have used SANS to measure the effect of the addition of small amounts of sodium dodecyl sulfonate (SDOS) on the size of C<sub>12</sub>EO<sub>8</sub> micelles (at a mole percent of SDOS of up to 4%). Consistent with our observations for SDS/C<sub>12</sub>EO<sub>6</sub>, the addition of small amounts of SDOS does not significantly alter the aggregation number but changes the inter-micellar interaction from an attractive to an increasingly repulsive one. For the 70/30 SDS/C<sub>12</sub>EO<sub>6</sub> composition, some additional measurements were made with reduced added electrolyte, and in this case, the inter-micellar interactions are increased and the micellar size is markedly reduced, consistent with other observations.<sup>22</sup> For the extreme composition of 5/95 (rich in C<sub>12</sub>EO<sub>6</sub>), some evidence of micellar growth and an elliptical rather than spherical shape is present. The micellar sizes are consistent with those measured previously for pure SDS<sup>22</sup> and C<sub>12</sub>EO<sub>6</sub>, C<sub>12</sub>EO<sub>8</sub>,<sup>42,43</sup> at low surfactant concentrations. Shiloach and Blankschtein<sup>9</sup> predicted SDS/C<sub>12</sub>EO<sub>6</sub> mixed micelles to be short cylinders from their molecular thermodynamics theory. From our results in a similar concentration and composition range to their calculations, there is little evidence for anything other than spherical micelles. Shiloach and Blankschtein<sup>44</sup> have more recently published an extensive comparison of the predictions of their molecular–thermodynamic theory with the measurements (by light scattering) of ionic/nonionic mixed micelle formation and growth. Their measurements on SDS/C<sub>12</sub>EO<sub>6</sub> are in general at higher concentrations than we have reported here and for solution compositions more rich in C<sub>12</sub>EO<sub>6</sub>. At higher C<sub>12</sub>EO<sub>6</sub> compositions ( $> 70$  mol %), they observe a growth of the mixed micelles, which has a maximum at a composition of 10% SDS. For solutions  $> 30$  mol % SDS, there is little change in the aggregation number with composition, and although their measurements were made at higher concentrations, their data in that region of solution compositions are consistent with our observations. Feitosu and Brown<sup>45</sup> have used dynamic light scattering to investigate mixed micelles of SDS/C<sub>12</sub>EO<sub>5</sub> over a wide concentration and composition range and observe an increase in hydrodynamic radius with increasing C<sub>12</sub>EO<sub>5</sub>/SDS ratio and with increasing temperature. Although this appears to be inconsistent with the C<sub>12</sub>EO<sub>6</sub>/SDS data, C<sub>12</sub>E<sub>5</sub> micelles have a greater tendency for growth with concentration and temperature (the clouding temperature is much closer to room temperature than for C<sub>12</sub>EO<sub>6</sub>).

In contrast to the SDS/C<sub>12</sub>EO<sub>6</sub> mixture, the C<sub>12</sub>EO<sub>6</sub>/C<sub>16</sub>TAB mixed surfactant micelles are much larger and grow with increasing concentration and C<sub>12</sub>EO<sub>6</sub> content in the solution (see Table 6 and Figures 5 and 7). For all but the lowest surfactant concentrations and for the micelles least rich in C<sub>16</sub>TAB, the micelles are now best described as ellipses with axial ratios from 1.3 to 3.3 and aggregation numbers from 120 to 250. At the

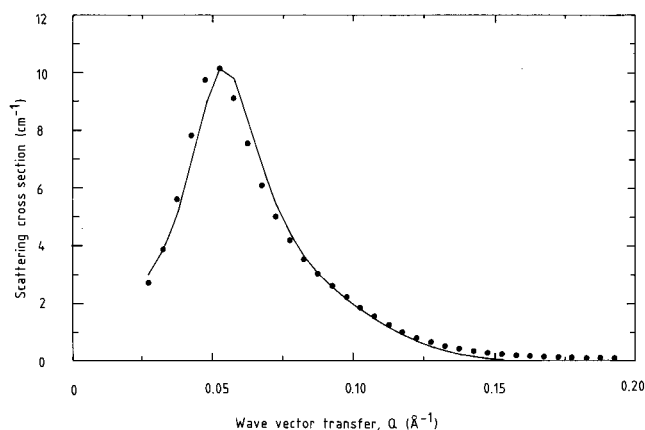


**Figure 6.** As in Figure 5 for hh/D<sub>2</sub>O, showing the best fit to polydisperse spheres.

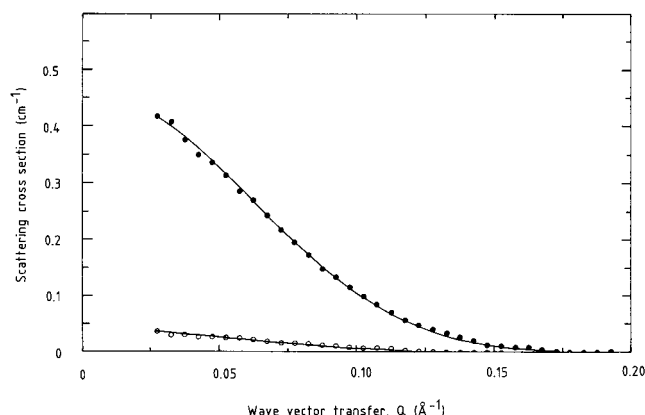


**Figure 7.** C<sub>16</sub>TAB ( $5 \times 10^{-3}$  M; 70/30)/C<sub>12</sub>EO<sub>6</sub>/NaCl (0.1 M) for hh (●) and dh (○) in D<sub>2</sub>O. The solid lines in Figures 3–7 are the calculated scattering curves for the model described in the text and using the parameters in Tables 5 and 6.

higher concentration (0.1 M), the scattering is also strongly dominated by the inter-micellar interactions (see Figure 5).

The 0.1 M 70/30 C<sub>16</sub>TAB/C<sub>12</sub>EO<sub>6</sub> data measured for h-C<sub>16</sub>TAB/h-C<sub>12</sub>EO<sub>6</sub> in D<sub>2</sub>O are particularly sensitive to the micellar shape, and Figure 6 shows the best fit obtained when the micelles are constrained to be spherical. In this case, the improvement in the model fit by allowing an elliptical distortion with an axial ratio of order 2.1 is self-evident. The micelle structural parameters obtained from C<sub>12</sub>EO<sub>6</sub>/C<sub>16</sub>TAB are entirely consistent with those obtained from pure C<sub>16</sub>TAB micelles<sup>22,46,47</sup> and their variation in growth with surfactant concentration.

For the C<sub>12</sub>EO<sub>6</sub>/C<sub>16</sub>TAB mixture, which mixes ideally, there is a marked change in micelle shape and size (aggregation number) with increasing concentration and C<sub>12</sub>EO<sub>6</sub> composition, whereas the SDS/C<sub>12</sub>EO<sub>6</sub> mixture, which departs from ideal mixing, shows no marked change in micelle size and shape with composition or concentration, except in the extreme C<sub>12</sub>EO<sub>6</sub> composition. The size and shape of the mixed SDS/C<sub>12</sub>EO<sub>6</sub> and C<sub>16</sub>TAB/C<sub>12</sub>EO<sub>6</sub> micelles and their variation with composition and concentration are consistent with the geometrical packing constraints developed by Isrealachvili et al.<sup>48</sup> The dimensionless packing parameter  $\nu/a_0l_c$  will determine the micelle shape (where  $\nu$  is the hydrocarbon volume,  $a_0$  the area per headgroup, and  $l_c$  the critical chain length): for  $\nu/a_0l_c < 1/3$ , spherical micelles will form, whereas for  $1/3 < \nu/a_0l_c < 1/2$ , nonspherical micelles exist. Increasing the chain length or reducing the headgroup size or area will induce micellar growth. For the SDS/C<sub>12</sub>EO<sub>6</sub> mixed micelles, the conditions for spherical micelles pertain, and even for increased C<sub>12</sub>EO<sub>6</sub> content, the reduction in  $a_0$  (due

to reduced SDS headgroup interactions) is not sufficient to promote growth. For C<sub>16</sub>TAB/C<sub>12</sub>EO<sub>6</sub>, the additional chain volume is sufficient (as for C<sub>16</sub>TAB alone) to more easily promote growth. Increasing the amount of C<sub>12</sub>EO<sub>6</sub> initially further enforces that tendency due to reduced C<sub>16</sub>TAB headgroup interactions, but at even higher C<sub>12</sub>EO<sub>6</sub> concentrations, the increased headgroup size of the nonionic causes a reduction in micellar size.

What is clear, however, from these results is that the micelle size and structure are dominated by these simple geometric packing constraints (as a single-component micelle) and that there is not a strong correlation between micelle size and any departure from ideality of mixing. Furthermore, any changes in mixing that depart from the regular solution approach and result in a nonzero excess entropy of mixing do not result in a measurable change in the structure of the mixed micelle, measurable by SANS.

## Summary

We have measured the composition and structure of mixed surfactant micelles over a wide range of solution compositions and concentrations for two nonionic–ionic surfactant mixtures, one that behaves ideally (C<sub>16</sub>TAB/C<sub>12</sub>EO<sub>6</sub>) and one that departs from ideal mixing (SDS/C<sub>12</sub>EO<sub>6</sub>). For the system (SDS/C<sub>12</sub>EO<sub>6</sub>) that mixes nonideally, the compositional data are broadly consistent with regular solution theory but in detail show some departure from theory. We attribute this to subtle changes in the packing of the two different surfactant components in the mixed micelle, as the overall structure and size of the SDS/C<sub>12</sub>EO<sub>6</sub> mixed surfactant micelles show no marked changes with composition or concentration. In contrast, for the surfactants that ideally mix, C<sub>16</sub>TAB/C<sub>12</sub>EO<sub>6</sub>, the mixed micelles show pronounced growth with increasing surfactant concentration and mole fraction of C<sub>12</sub>EO<sub>6</sub> in solution. We conclude that for both of these systems, there is not a strong correlation between micelle size and structure and ideality of mixing.

**Acknowledgment.** We acknowledge the contribution of the instrument scientists at ISIS (S. King and R. K. Heenan) and at ILL (S. Egelhaff and E. Bellet-Amalric) in obtaining the SANS data reported in this paper.

## References and Notes

- (1) Scaemhorn, J. F. In *Mixed Surfactant Systems*; Ogino, K., Abe, M., Eds.; Marcel Dekker: New York, 1992.
- (2) Rosen, M. In *Phenomena in mixed surfactant systems*; Scaemhorn, J. F., Eds.; ACS Symposium Series 311; American Chemical Society: Washington, DC, 1988.
- (3) Clint, J. H. *J. Chem. Soc., Faraday Trans. 1* **1975**, 71, 1327.
- (4) Rubingh, D. N. In *Solution Chemistry of Surfactants*; Mittal, K., Ed.; Plenum: New York, 1979; Vol. 1.
- (5) Rubingh, D. N.; Holland, P. M. In *Cationic Surfactants, Physical Chemistry*; Rubingh, D. N., Holland, P. M., Eds.; Surfactant Science Series 37; Marcel Dekker: New York, 1990.
- (6) Puvvada, S.; Blankschtein, D. *J. Phys. Chem.* **1992**, 96, 5579.
- (7) Sarmoria, C.; Puvvada, S.; Blankschtein, D. *Langmuir* **1992**, 8, 2690.
- (8) Zoeller, N. J.; Shiloach, A.; Blankschtein, D. *Chemtech* **1996**, 26 (3), 24.
- (9) Shiloach, A.; Blankschtein, D. *Langmuir* **1997**, 14, 1618.
- (10) Thomas, H. G.; Lomatin, A.; Blankschtein, D.; Benedek, G. D. *Langmuir* **1997**, 13, 209.
- (11) Penfold, J.; Staples, E.; Thompson, L.; Tucker, I.; Hines, J.; Thomas, R. K.; Lu, J. R. *Langmuir* **1995**, 11, 2496.
- (12) Pedone, L.; Chillura Martino, N.; Caponetti, E.; Floriano, M. A.; Triolo, R. *J. Phys. Chem. B* **1997**, 101, 9525.
- (13) Brasher, L. L.; Kaler, E. W. *Langmuir* **1996**, 12, 6270.
- (14) Griffiths, P. C.; Stilbs, P.; Paulsen, K.; Howe, A. M.; Pitt, A. R. *J. Phys. Chem. B* **1997**, 101, 915.



- (15) Zana, R.; Lévy, H.; Danino, D.; Talmon, Y.; Kwetkat, K. *Langmuir* **1997**, *13*, 402.
- (16) Staples, E.; Thompson, L.; Tucker, I.; Thomas, R. K.; Lu, J. R. *Langmuir* **1993**, *9*, 165.
- (17) Staples, E.; Thompson, L.; Tucker, I.; Penfold, J. *Langmuir* **1994**, *10*, 4136.
- (18) Penfold, J.; Staples, E.; Thompson, L.; Tucker, I. *Colloid Surf.* **1995**, *102*, 127.
- (19) Penfold, J.; Staples, E.; Cummins, P.; Tucker, I.; Thomas, R. K.; Simister, E. A.; Lu, J. R. *J. Chem. Soc., Faraday Trans.* **1996**, *92*, 1773.
- (20) Penfold, J.; Staples, E.; Cummins, P.; Tucker, I.; Thomas, R. K.; Simister, E. A.; Lu, J. R. *J. Chem. Soc., Faraday Trans.* **1996**, *92*, 403.
- (21) Penfold, J.; Staples, E.; Tucker, I.; Thomas, R. K. *J. Colloid Interface Sci.* **1998**, *201*, 223.
- (22) Hayter, J. B.; Penfold, J. *J. Colloid Polym. Sci.* **1983**, *261*, 1072.
- (23) Simister, E. A.; Thomas, R. K.; Penfold, J.; Aveyard, R.; Binks, B. P.; Fletcher, P. D. I.; Lu, J. R.; Sokolowski, A. *J. Phys. Chem.* **1992**, *96*, 1383.
- (24) Lu, J. R.; Lee, E. M.; Thomas, R. K.; Penfold, J.; Flitsch, S. L. *Langmuir* **1993**, *9*, 1352.
- (25) Heenan, R. K.; King, S. M.; Penfold, J. *J. Appl. Crystallogr.* **1997**, *30*, 1140.
- (26) Neutron Beam Facilities at the high flux reactor available for users. Institute Laue Langevin, Grenoble, France, 1994.
- (27) Heenan, R. K.; King, S. M.; Osborn, R.; Stanley, H. B. *RAL Int. Rep.* **1989**, RAL-89-128.
- (28) Ghosh, R. E. *Institute Laue Langevin Internal Report*, 81GH297, 1981.
- (29) Hayter, J. B. In *Physics of Amphiphiles, Micelles, Vesicles and Microemulsions*; Degiorgio, V., Corti, M., Eds.; North-Holland: Amsterdam, 1992.
- (30) Hayter, J. B.; Penfold, J. *Mol. Phys.* **1981**, *42*, 109.
- (31) Hayter, J. B.; Hansen, J. B. *Mol. Phys.* **1982**, *42*, 651.
- (32) Hoffmann, H.; Poesnecker, G. *Langmuir* **1994**, *10*, 381.
- (33) Hines, J. D.; Thomas, R. K.; Garrett, P. R.; Rennie, G. K.; Penfold, J. *J. Phys. Chem. B* **1998**, *102*, 8834.
- (34) Hines, J. D.; Thomas, R. K.; Garrett, P. R.; Rennie, G. K.; Penfold, J. *J. Phys. Chem. B* **1997**, *101*, 9215.
- (35) Baglioni, P.; Dei, L.; Rivara-Minten, E.; Kevan, L. *J. Am. Chem. Soc.* **1993**, *115*, 4286.
- (36) Davidson, C. J. Ph.D. Thesis, University of Aberdeen, Aug 1983.
- (37) Takisawas, N.; Brown, P.; Bloor, D. M.; Hall, D. G.; Wyn-Jones, E. *J. Chem. Soc., Faraday Trans.* **1989**, *85*, 2099.
- (38) Griffiths, P. C.; Stilbs, P.; Paulsen, K.; Howe, A. M.; Pitt, A. R. *J. Phys. Chem. B* **1997**, *101*, 915.
- (39) Ciccareli, D.; Cosantino, L.; D'Errico, G.; Pacluano, L.; Vitagliano, V. *Langmuir* **1998**, *14*, 7130.
- (40) Hassan, P. A.; Bhagwat, S. S.; Manohar, C. *Langmuir* **1995**, *11*, 470.
- (41) Douglas, C. B.; Kaler, E. W. *Langmuir* **1994**, *10*, 1075.
- (42) Magid, L. J.; Triolo, R.; Johnson, J. S. *J. Phys. Chem.* **1984**, *88*, 3730.
- (43) Zulauf, M.; Weckstrom, H.; Hayter, J. B.; Degiorgio, V.; Corti, M. *J. Phys. Chem.* **1985**, *89*, 3411.
- (44) Shiloach, A.; Blankenshtein, D. *Langmuir* **1997**, *13*, 3968.
- (45) Feitosu, E.; Brown, W. *Langmuir* **1998**, *14*, 4460.
- (46) Quirion, F.; Magid, L. J. *J. Phys. Chem.* **1986**, *90*, 5435.
- (47) Berr, S. *J. Phys. Chem.* **1987**, *91*, 4766.
- (48) Isrealachvili, J. N.; Mitchell, C. J.; Ninhan, B. W. *J. Chem. Soc., Faraday Trans. 1* **1976**, *72*, 1525.
- (49) Barzykin, A. V.; Almgren, M. *Langmuir* **1996**, *12*, 4672.